Journal of Bioenergetics and Biomembranes, Vol. 34, No. 4, August 2002 (© 2002)

Proteolytic Modification of Swelling-Activated Cl^- Current in LNCaP Prostate Cancer Epithelial Cells

Yulia V. Vitko,[1] Nelli H. Pogorelaya,[2] Natalia Prevarskaya,[3] Roman Skryma,[3] and Yaroslav M. Shuba[1,4]

Received February 20, 2002; accepted June 5, 2002

The effects of intracellular application of trypsin on the Cl^- current induced by hypotonic cell swelling ($I_{Cl,swell}$) in human prostate cancer epithelial cells (LNCaP) was studied using the patch-clamp technique. In cells predialyzed with 1 mg/mL trypsin, $I_{Cl,swell}$ developed and diminished in response to the application and withdrawal of hypotonic solution about three times faster than that in control cells. In trypsin-infused cells, $I_{Cl,swell}$ also had about twofold higher current density and displayed considerably slowed voltage-dependent inactivation, which was quite pronounced in control cells at potentials above +60 mV. Trypsin-induced modification of $I_{Cl,swell}$ could be prevented by coinfusion of 10 mg/mL soybean trypsin inhibitor, suggesting that proteolytic cleavage of essential intracellular structural domains of the $I_{Cl,swell}$-carrying volume-regulated anion channel (VRAC) was responsible for this functional modification. The effect of trypsin was not dependent on the presence of intracellular ATP. We conclude that VRACs, similarly to voltage-gated Na^+, K^+, and Cl^- channels, possess intracellular inactivation domain(s) subjected to proteolytic cleavage that may function in conformity with the classical "ball-and-chain" inactivation model.

KEY WORDS: LNCaP prostate cancer cells; swelling-activated Cl^- current; trypsin; voltage-dependent inactivation.

INTRODUCTION

Although various membrane ion channels are characterized by quite diverse primary mechanisms that turn them on and off, nevertheless most of them possess at least some kind of voltage-dependent gating as well. Voltage-dependent ion channels (Na^+, Ca^{2+}, K^+), whose operational mode is solely determined by membrane voltage, represent the extreme case of such gating. Early biophysical studies postulated the existence in this type of ion channels of at least three functional domains that must govern their gating: voltage sensor, activation gates, and inactivation gates. The first experimental evidence that provided structural basis for the presence of such functional domains came from the studies on the prevention of inactivation (the process that refers to the closing of channels during sustained depolarization) in Na^+ channels by intracellular application of proteolytic enzymes (Armstrong *et al.*, 1973). These results were interpreted in terms of the existence of a specific structural entity on the inner surface of the Na^+ channel, responsible for inactivation, which is cleaved by proteolytic treatment, leading to the loss of inactivation. It was hypothesized that this entity consisted of a particle (termed the "ball"), tethered to the inner surface of the channel by a "chain," which is able to block the channel pore via interaction with the receptor site in its inner vestibule ("ball-and-chain" model; Armstrong, 1981; Bezanilla and Armstrong, 1977). Removal of inactivation in response to the intracellular infusion of trypsin was also documented for L-type Ca^{2+} (Hescheler and Trautwein, 1988; Shuba *et al.*, 1990) and

[1] Bogomoletz Institute of Physiology, Bogomoletz Street, 4, 01024 Kiev-24, Ukraine.
[2] International Centre of Molecular Physiology NASU, Bogomoletz Street, 4, 01024 Kiev-24, Ukraine.
[3] Laboratoire de Physiologie Cellulaire, INSERM EPI 9807, Bât. SN3, Université des Sciences et Technologies de Lille, 59655 Villeneuve d' Ascq, France.
[4] To whom correspondence should be addressed; e-mail: yshuba@serv.biph.kiev.ua.

0145-479X/02/0800-0307/0

K^+ (Mayorga-Wark *et al.*, 1993; Solaro and Lingle, 1992; Zagotta *et al.*, 1990) channels, suggesting that modification of inactivation by proteolytic enzymes can be generally viewed as evidence for the existence of specialized intracellular determinants responsible for the channel's voltage-dependent inactivation.

Purification, molecular cloning, and structure-functional studies of the principal $\alpha 1$ subunits of Na^+, Ca^{2+}, and K^+ channels have provided a molecular basis for the physical identification of various structural domains, including those governing voltage-dependent inactivation. Moreover, molecular groups facing the cytosol, implicated in the voltage-dependent inactivation of Na^+ and K^+ channels, have indeed been proven to function in conformity with the ball-and-chain or "hinged-lid" models (Hoshi *et al.*, 1990; for reviews see Armstrong and Hille, 1998; Catterall, 1996).

Although the chloride current activated in response to cell swelling ($I_{Cl,swell}$) differs drastically from currents passing through the voltage-gated ion channels in terms of the activation mechanism, it exhibits pronounced inactivation at high positive potentials (above +60 mV) (e.g., Jackson and Strange, 1995; Kubo and Okada, 1992; Levitan and Garber, 1995; for review, see Okada, 1997). This current is widely repreented in many cell types and is critically involved in regulatory volume decrease (RVD) (for reviews, see Nilius *et al.*, 1997; Okada, 1997; Strange *et al.*, 1996).

The molecular nature of the volume-regulated anion channel (VRAC) underlying $I_{Cl,swell}$ is still unknown, which impedes identification of the structural parts responsible for its specific properties, including inactivation. Inactivation of $I_{Cl,swell}$ is considered to be voltage-dependent in nature, although no evidence of the specialized inactivation domain(s) in VRAC has yet been presented. The existence of some endogenous regulatory factor(s) that may take part and/or induce inactivation of VRAC is, therefore, still a possibility. Although membrane potentials at which $I_{Cl,swell}$ inactivates are quite high, suggesting that this process does not play a substantial role in its physiological function, further study of inactivation may shed some light on the molecular organization of VRAC.

We recently described VRAC-mediated $I_{Cl,swell}$ in a human prostate cancer epithelial cell line, LNCaP (Lymph Node Carcinoma of the Prostate) (Shuba *et al.*, 2000), and showed its peculiar regulation by Ca^{2+} (Lemonnier *et al.*, 2002). Here we focused on examining the effects of intracellular application of trypsin on the properties of $I_{Cl,swell}$ in these cells. Our data suggest the existence in VRAC of structural intracellular inactivation domain(s), cleavage of which by the enzyme not only removes $I_{Cl,swell}$ inactivation but also changes the characteristics of current activation by cell swelling.

METHODS

Cell Cultures

The procedure of culturing LNCaP cells was described elsewhere (Shuba *et al.*, 2000).

Electrophysiology and Solutions

Macroscopic membrane ionic currents in LNCaP cells (average whole-cell membrane capacitance, $C_m = 25.5 \pm 1.2$ pF, $n = 46$) were recorded in the whole-cell configuration of the patch-clamp technique with a PC-ONE amplifier (Dagan Inc., U.S.A.). As LNCaP cells possess a voltage-activated, TEA-sensitive, K^+ current (Skryma *et al.*, 1997), we used TEA as a major cation in our experimental extracellular solutions to prevent $I_{Cl,swell}$ contamination with this current. The compositions of the normal and TEA-based isotonic (310 mosmol/l) and hypotonic (190 mosmol/l) extracellular solutions are presented in Table I. The basic intracellular pipette solution (osmolarity 290 mosmol/l) contained (in mM): K-gluconate, 100; KCl, 40; $MgCl_2$, 1; $CaCl_2$, 0.5; HEPES, 10; EGTA, 10; Mg-ATP, 5; pH, 7.2. The resistance of the pipette varied between 3 and 5 MΩ, and series resistance compensation was used to improve voltage-clamp performance. A total of 1 mg/mL trypsin (type II-S, Sigma) and 10 mg/mL soybean trypsin inhibitor (type II-S, Sigma) were added directly to the intracellular solution without significantly changing its osmolarity. External solutions were changed using a multibarrel puffing micropipette with common

Table I. Composition of the Extracellular Solutions

	Normal	iso-TEA	hypo-TEA
NaCl	140	—	—
KCl	5	—	—
$CaCl_2$	2	2	2
$MgCl_2$	2	2	2
Na_2HPO_4	0.3	—	—
KH_2PO_4	0.4	—	—
$NaHCO_3$	4	—	—
Glucose	5	5	5
HEPES	10	10	10
TEA-Cl	—	145	84

Note. Concentration is given in mM. pH of all solutions was adjusted to 7.3.

outflow, positioned in close proximity to the cell under investigation. During the experiment, the cell was continuously superfused with the solution via puffing pipette to reduce possible artefacts related to the switches from static to moving solution and vice versa. Complete external solution exchange was achieved in less than 1 s.

Data Analysis and Statistics

Each experiment was repeated several times. The data were analyzed using pCLAMP 6 (Axon Instr., Foster City, CA) and Origin 5.0 (Microcal, Northhampton, MA) software. Results were expressed as mean ± standard error of the mean (SE) where appropriate. Student's *t* test was used for statistical comparison of the differences, with $P < 0.05$ considered to be significant. Characteristic times of $I_{Cl,swell}$ development and diminution were determined as follows: the time interval from the application of hypotonic solution till the current reached 0.05 ($A_{max} - A_{base}$) was considered as the latency (or delay) period (T_{lat}), the time interval during which the current changed from 0.05 ($A_{max} - A_{base}$) to 0.95 ($A_{max} - A_{base}$) was considered as current development period (T_{dev}), while the time interval during which the current decreased from 0.95 ($A_{max} - A_{res}$) to 0.05 ($A_{max} - A_{res}$) following return to isotonic solution was considered as the diminution period (T_{dim}) (here A_{base} is the baseline current before hypotonic exposure, A_{max} is the maximum amplitude of hypotonicity-evoked $I_{Cl,swell}$, and A_{res} is the amplitude of residual $I_{Cl,swell}$ after the return to isotonicity).

RESULTS

Baseline Properties of $I_{Cl,swell}$

Under whole-cell patch-clamp recording with standard intracellular solution in the pipette LNCaP cells responded to hypotonic exposure by generating an outwardly rectifying current, which had a reversal potential, $V_r = -20 \pm 4$ mV, closely matching the equilibrium potential for Cl^- ions (Fig. 1(A)). Following application of hypotonic solution, this current $I_{Cl,swell}$ started to develop after a latency period of 93 ± 38 s (Fig. 1(C) and (D)) and reached maximum density of 63 ± 7 pA/pF at +100 mV (Fig. 1(B)) within the next 298 ± 55 s (Fig. 1(C) and (D)), whereas a return to the isotonic solution resulted in quite fast, virtually complete diminution of $I_{Cl,swell}$ within 103 ± 28 s (Fig. 1(C) and (D)).

At step depolarizations above +60 mV, the fully developed $I_{Cl,swell}$ showed time-dependent inactivation, at a rate which increased as depolarization became more positive (Fig. 2(A)). At pulse potential +120 mV, the current waveform could be represented as the sum of exponentially decaying and sustained components (Fig. 2(B)). The time constant of the exponential component (τ_{in}) was 67 ± 5 ms while its amplitude (A_{exp}) exceeded that of the sustained component (A_{sus}) by about fivefold (Fig. 2(B) and (C)). Since $I_{Cl,swell}$ did not exhibit any signs of voltage-dependent activation, whereas inactivation was quite slow, the I-V relationship of the peak current (Fig. 2(D), gray squares) could be viewed as not appreciably affected by any of these processes. On the other hand, the I-V relationship of the sustained current (Fig. 2(D), open squares, determined from exponential fit) was dependent not only on the driving force for Cl^- but also on the level of steady-state inactivation. Therefore, by dividing the "sustained" I-V by the "peak" I-V (see Fig. 2(D)) it was possible to obtain the $I_{Cl,swell}$ steady-state inactivation dependency, an example of which for a representative LNCaP cell is presented in Fig. 2(F) (open squares). The fit of this dependency with the Bolzmann equation (see legend to Fig. 2) made it possible to determine parameters of steady-state inactivation of the control $I_{Cl,swell}$, such as half inactivation potential, $V_{1/2} = +58.3$ mV, slope factor (determined by the effective charge of the gating particle), $k = -15.5$ mV, and the minimum inactivation level, $I_{min} = 0.15$.

Effects of Intracellular Trypsin on $I_{Cl,swell}$

Inclusion of 1 mg/mL trypsin in the patch pipette did not produce visible changes in the baseline current under isotonic conditions within about 10 min of dialysis (Fig. 1(A), inset). Since trypsin is a rather big molecule with molecular mass $m = 20$ kDa, we usually waited at least 8 min before any intervention was administered to ensure that its concentration within the cell equilibrated to that in the pipette. According to studies by Push and Neher (1988), the time constant τ (in s) of the exponential rise in concentration within the cell of the pipette constituent with molecular mass m (in Da) is related to the access resistance of the pipette R_a (in MΩ), and cell volume V (in μm^3) according to the following empirical equation:

$$\tau = 0.6 \times R_a \times m^{1/3} \times V \times 1897^{-1}.$$

Quantitative estimates for the typical volume of an LNCaP cell $V = 4000$ μm^3 and access resistance of the pipette $R_a = 6$ MΩ (R_a is generally higher than just the resistance of cellfree pipette) yielded the τ value for trypsin of about 3.5 min. Thus, 8-min dialysis should provide sufficient time to achieve a trypsin concentration within the cell basically equal to that in the pipette.

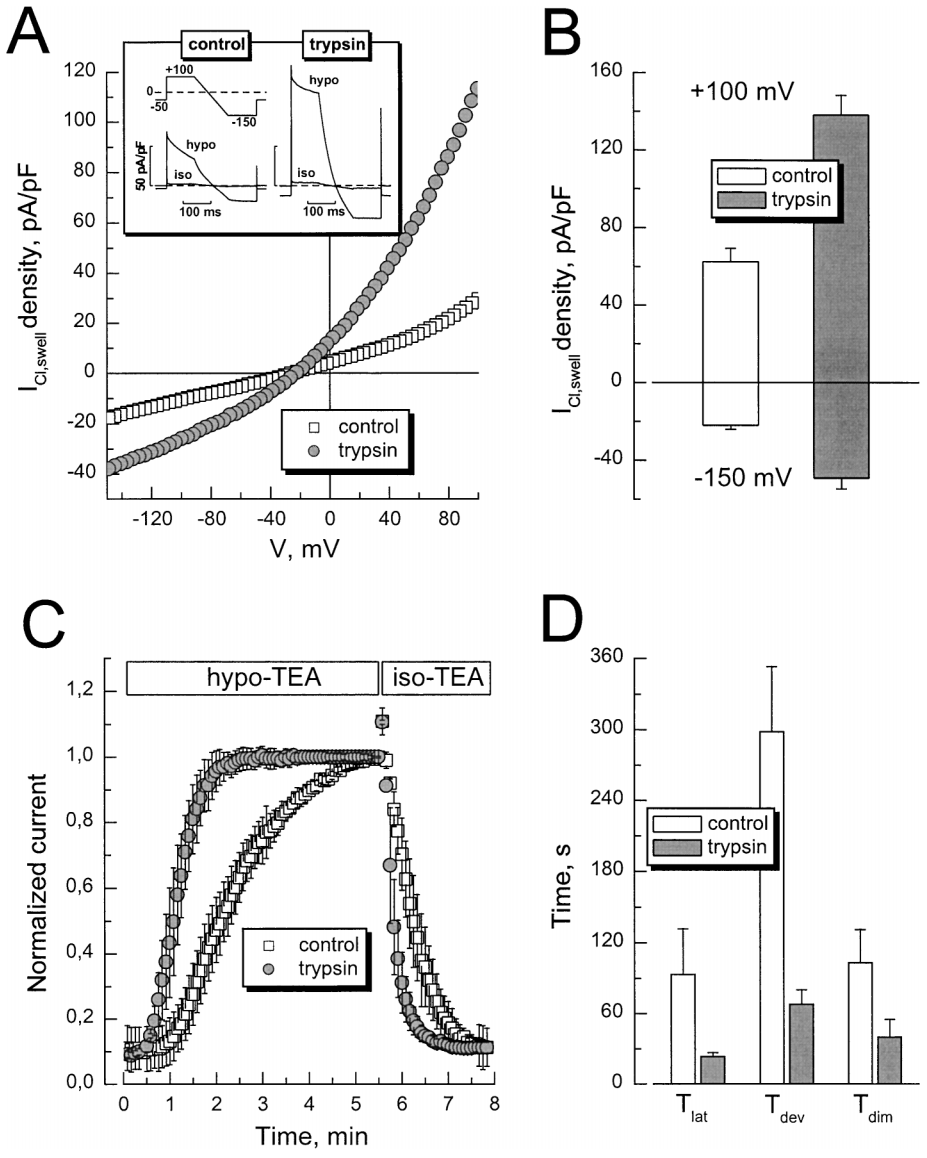

Fig. 1. Intracellular trypsin enhances volume sensitivity and increases amplitude of $I_{Cl,swell}$ in LNCaP prostate cancer epithelial cells. (A) Representative I-V relationships of $I_{Cl,swell}$ obtained in control (open squares) and trypsin-infused (gray circles) cells; the inset demonstrates original tracings of the baseline current (iso) and fully developed $I_{Cl,swell}$ (hypo) acquired from respective cells, using the depicted voltage-ramp pulse protocol, the ramp portions of which were used to derive the I-Vs. (B) Bar graph showing the difference in $I_{Cl,swell}$ densities between control (white column) and trypsin-infused (gray column) cells at indicated membrane potentials (mean $\pm$ SE, $n = 10$ for each cell type). (C) Normalized and averaged time courses (mean $\pm$ SE, $n = 10$, for each cell type). of $I_{Cl,swell}$ development and diminution in response to changes in extracellular tonicity (shown on top) in control (open squares) and trypsin-infused (gray circles) cells; (D) quantification of the latency (T_{lat}), development (T_{dev}) and diminution (T_{dim}) periods of $I_{Cl,swell}$ in response to change in extracellular tonicity in control (white columns) and trypsin-infused (gray columns) cells (mean $\pm$ SE, $n = 10$, for each cell type).

In the presence of intracellular trypsin, LNCaP cells responded to hypotonic exposure by generating current with the same reversal potential as control $I_{Cl,swell}$ (Fig. 1(A)), but with quite different parameters of development and inactivation as well as maximum amplitude. Figure 1(C) compares averaged normalized time courses of $I_{Cl,swell}$ in response to variations in extracellular osmolarity in control and trypsin-infused LNCaP cells. Inspection of these time courses as well as quantification of the latency (T_{lat}), current development (T_{dev}), and current diminution (T_{dim}) periods (Fig. 1(D)) suggests that intracellular trypsin leads to substantial acceleration of $I_{Cl,swell}$

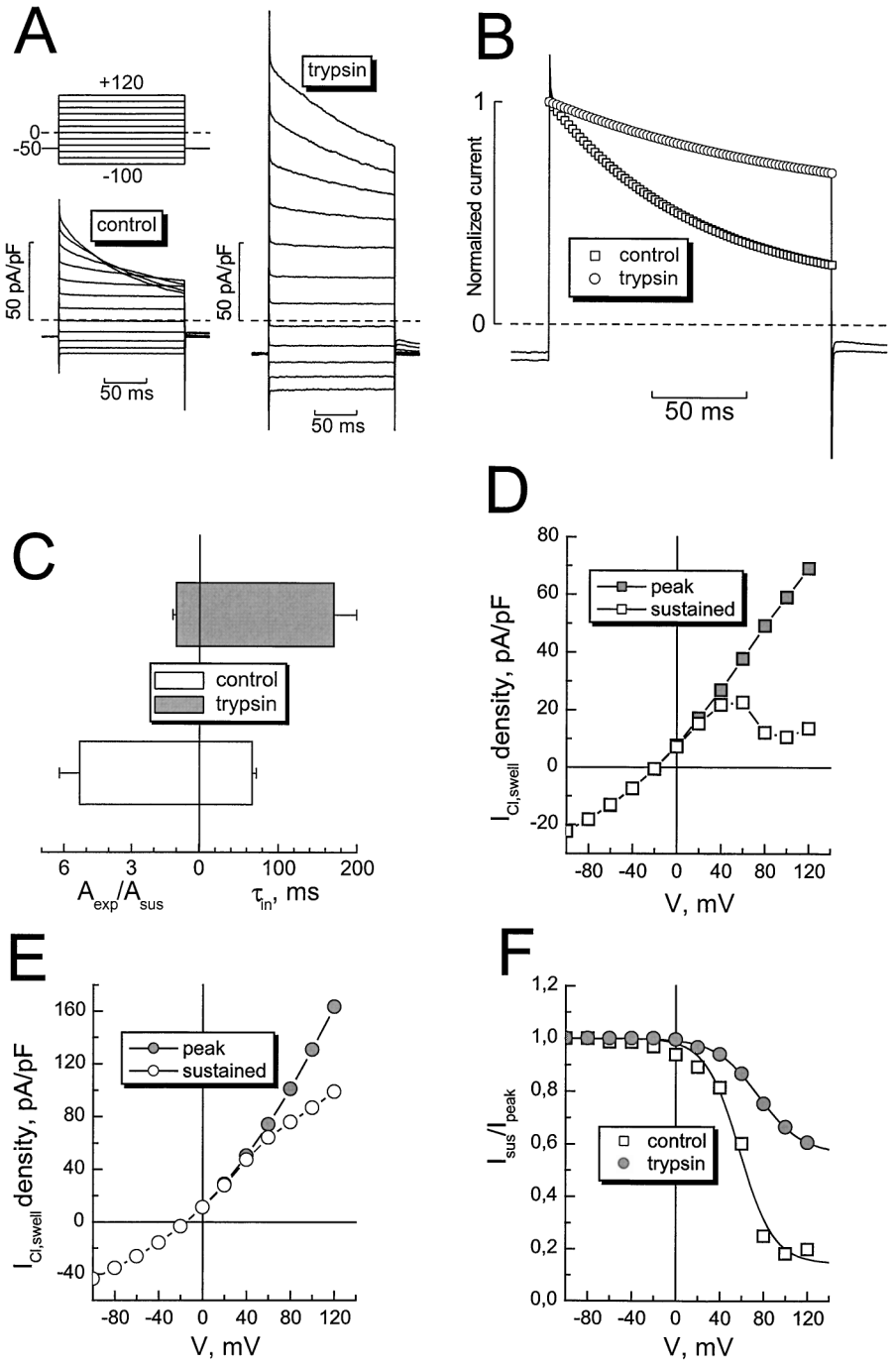

Fig. 2. Intracellular trypsin modifies voltage-dependent inactivation of $I_{\mathrm{Cl,swell}}$ in LNCaP prostate cancer epithelial cells. (A) Representative tracings of fully developed $I_{\mathrm{Cl,swell}}$ obtained in control and trypsin-infused cells in response to the depicted pulse protocol (above control traces). (B) normalized currents at pulse potential +120 mV with superimposed exponential fits of the decay phases for control (squares, $\tau_{\mathrm{in}} = 72$ ms) and trypsin-infused (circles, $\tau_{\mathrm{in}} = 148$ ms) cells. (C) Quantification of the time constants of inactivation (τ_{in}) and of the ratios between the amplitudes of the exponentially decaying (A_{exp}) and sustained (A_{sus}) components of control (white bars) and trypsin-modified (gray bars) $I_{\mathrm{Cl,swell}}$ at +120 mV (mean ± SE, $n = 10$, for each cell type). (D, E) I-V relationships of the peak $I_{\mathrm{Cl,swell}}$ (gray symbols) and of its sustained components (open symbols) in representative control (D) and trypsin-infused (E) cells. (F) steady-state inactivation dependencies of control (open squares) and trypsin-modified (gray circles) $I_{\mathrm{Cl,swell}}$ derived from the I-Vs presented on panels (D) and (E) respectively; continuous lines represent the best fits of the data points with the Bolzmann equation: $I_{\mathrm{sus}}/I_{\mathrm{peak}} = 1 - (1 - I_{\mathrm{min}})/(1 + \exp(V - V_{1/2})/k))$,

with half inactivation potential, $V_{1/2}$, constituting +58.3 mV and = +75.2 mV, slope factor, k, −15.5 and −19.7 mV, and the minimum inactivation level, I_{min}, −0.15 and 0.57 for control and trypsin-modified currents, respectively.

responses to changes in extracellular osmolarity. In the presence of intracellular trypsin, the first two characteristic times were shortened by a factor of about 4 and the third by a factor of 2.5, compared to control (T_{lat} from 93 ± 38 to 23 ± 3 s, T_{dev} from 298 ± 55 to 68 ± 12 s, and T_{dim} from 103 ± 28 to 40 ± 15 s, see Fig. 1(D)).

Trypsin infusion also resulted in an increase of about twofold in maximum $I_{Cl,swell}$ density (Fig. 1(B)) and a significant slowing of current inactivation at high positive potentials (Fig. 2(A) and (B)). Figure 2(B) compares normalized representative traces of $I_{Cl,swell}$ at +120 mV from control and trypsin-infused cells. Exponential quantification of the decay phases of these currents suggests that the apparent slowing of inactivation by intracellular trypsin is due to substantial prolongation of the time constant (τ_{in}) of the exponentially decaying component (from 67 ± 5 to 170 ± 29 ms) accompanied by a decrease in its amplitude (A_{exp}) and a simultaneous enhancement of the sustained current amplitude (A_{sus}), such that contribution of both to the overall $I_{Cl,swell}$ became nearly equal (Fig. 2(B) and (C)).

The Bolzmann fit of the steady-state inactivation dependency of trypsin-modified $I_{Cl,swell}$ (Fig. 2(F), grey circles) derived from the ratio of its "sustained" and "peak" I-Vs (Fig. 2(E)) showed that such a modification also resulted in a positive shift of almost 20 mV in the half inactivation potential (to $V_{1/2} = +75.2$ mV), an increase of nearly 30% in the absolute value of slope factor (to $k = -19.7$ mV), and an increase of about fourfold in the minimum inactivation level (to $I_{min} = 0.57$), compared to the control.

Addition of 10 mg/mL soybean trypsin inhibitor to the pipette solution containing 1 mg/mL trypsin prevented proteolytic modification of $I_{Cl,swell}$, such that all the major parameters described earlier remained similar to those of the control. This is evidenced in part by Figs. 3(A) and (B), which compare the time courses of $I_{Cl,swell}$ development and diminution in response to changes in extracellular osmolarity (Fig. 3(A)) and inactivation of fully developed $I_{Cl,swell}$ at +120 mV (Fig. 3(B)) in the representative control and trypsin-plus-inhibitor infused LNCaP cells. Suppression of the trypsin effects on $I_{Cl,swell}$ by the trypsin inhibitor suggests that these effects are indeed related to the proteolytic activity of the enzyme.

Effect of Trypsin on $I_{Cl,swell}$ is Not Modulated by Intracellular ATP

It is generally accepted that the activity of the VRACs that carry $I_{Cl,swell}$ is dependent on intracellular ATP (reviewed by Okada, 1997) although simple removal of ATP from the pipette solution is not usually sufficient to demonstrate the ATP-dependence of $I_{Cl,swell}$ and additional use of metabolic inhibitors is required (e.g., Jackson *et al.*, 1994; Meyer and Korbmacher, 1996; Oiki *et al.*, 1994). To determine whether the upregulating effects of trypsin on $I_{Cl,swell}$ described thus far are related to intracellular ATP to any extent, we conducted a series of experiments using ATP-free intracellular pipette solution. As was already mentioned, cell dialysis with trypsin-supplemented pipette solutions continued for at least 8 min prior to hypotonic exposure. Since ATP is rather small molecule such prolonged dialysis ensured that depending on whether or not ATP is present in the pipette the endogenous ATP would be either washed out or replaced by the exogenous one. Figures 3(C) and (D) show that the time course of $I_{Cl,swell}$ development and diminution (Fig. 3(C)) was independent of the intracellular ATP level in two representative LNCaP cells. The current waveform at +120 mV (Fig. 3(D)) also remained basically the same. Quantification of the mean parameters of $I_{Cl,swell}$ in the cells dialyzed with and without ATP in the presence of trypsin did not reveal any statistically significant differences either (data not shown), suggesting that intracellular ATP is not important for trypsin-mediated modification of $I_{Cl,swell}$.

DISCUSSION

In this study, we report for the first time on the effects of intracellular endoprotease trypsin on swelling-activated chloride current, $I_{Cl,swell}$, in LNCaP prostate cancer epithelial cells and show that intracellular administration of this enzyme results in (i) acceleration of $I_{Cl,swell}$ responses to changes in extracellular osmolarity, (ii) suppression of $I_{Cl,swell}$ inactivation, and (iii) increase in $I_{Cl,swell}$ amplitude. Proteolytic modification had previously been described in voltage-dependent Na^+ (e.g., Armstrong *et al.*, 1973; Gonoi and Hille, 1987), K^+ (Mayorga-Wark *et al.*, 1993; Solaro and Lingle, 1992; Zagotta *et al.*, 1990), and L-type Ca^{2+} currents (Hescheler and Trautwein, 1988; Shuba *et al.*, 1990.). The primary feature of this modification is the dramatic slowing of current inactivation, often accompanied by potentiation of the current amplitude (Gonoi and Hille, 1987). However, the progressive rundown of Na^+ current during protease-induced slowing of inactivation observed in giant squid axons (e.g., Armstrong *et al.*, 1973) as well as the decoupling of the processes of L-type Ca^{2+} current augmentation in time and the slowing of inactivation (Hescheler and Trautwein, 1988) suggests that inactivation gates are not the only structures affected by enzyme treatment and that some other important determinants may also be affected.

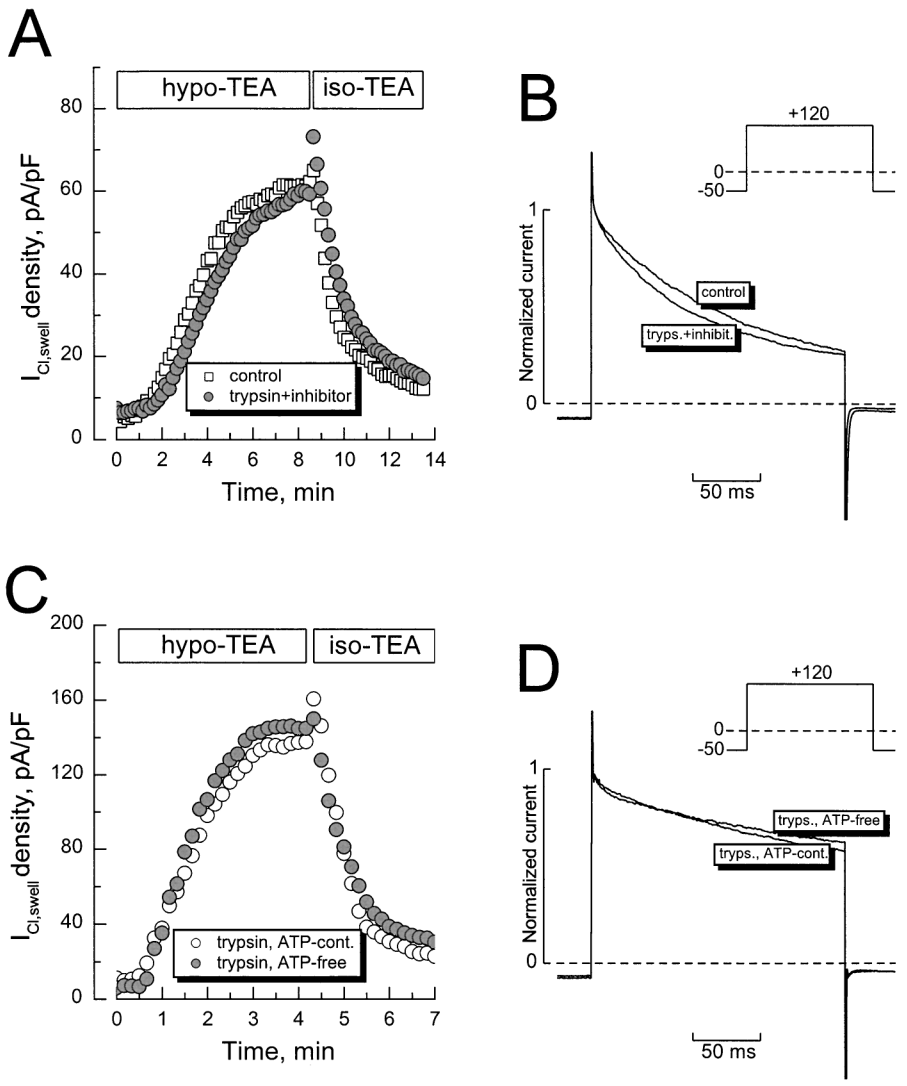

Fig. 3. The effects of intracellular trypsin are abolished by a trypsin inhibitor and are not dependent on intracellular ATP. (A, B) comparison of the time courses of $I_{Cl,swell}$ development and diminution in response to changes in extracellular tonicity (shown on top) (A) and of normalized original currents (B) pulse protocol is depicted in the inset in a representative control LNCaP cell and an LNCaP cell infused with a mixture of trypsin (1 mg/mL) and trypsin inhibitor (10 mg/mL), showing virtually no difference in either the time courses or the kinetics of $I_{Cl,swell}$. (C, D) same as in (A) and (B) respectively, but for two representative LNCaP cells infused with trypsin in the absence of ATP (ATP-free) or in the presence of 5 mM Mg-ATP (ATP-cont.) in the pipette solution.

Structure functional studies of cloned Na^+ channel $\alpha 1$ subunits have identified the intracellular loop between domains III and IV as the inactivation gate that occludes the pore via interaction of its three-residue cluster, comprising the inactivation particle with the receptor site on the channel inner vestibule (Stühmer *et al.*, 1989; Vassilev *et al.*, 1988). As the loop implicated in Na^+ channel inactivation is quite short, placing the inactivation particle very close to the inner mouth of the pore, from a mechanistic point of view, Na^+ channel inactivation is more adequately described by the hinged-lid rather than the ball-and-chain model (Catterall, 1996).

Although the primary $\alpha 1$ subunits of Na^+ and Ca^{2+} channels have similar structures, no evidence has been obtained for the role of III and IV linker or any other cytoplasmic loop or terminus in voltage-dependent inactivation of Ca^{2+} channels. Instead, and quite unexpectedly, voltage-dependent inactivation of Ca^{2+} channels was traced to the membrane-spanning segment S6 of homologous domain I and its flanking regions (Zhang *et al.*, 1994). On the contrary, structural regions of the Ca^{2+} channel $\alpha 1$

subunit involved in specific Ca^{2+}-dependent inactivation are distributed among several cytoplasmic domains including the I-II and II-III loops and the C terminus (Adams and Tanabe, 1997).

Voltage-dependent inactivation of K^+ channels seems to correspond best to the classical ball-and-chain mechanism. Using *Shaker* B K^+ channel as the model for studying voltage-dependent inactivation, it was shown that the first 20 residues of its N terminus represented an inactivation particle ("ball") attached to the "chain" composed of the next 63 residues (Hoshi *et al.*, 1990).

Thus, while molecular substrates for proteolytic modification of voltage-dependent inactivation can easily be identified in Na^+ and K^+ channels, this is not so easy in Ca^{2+} channels. The primary targets for proteolytic modification of Ca^{2+} channels may be intracellularly exposed groups involved in Ca^{2+}-dependent inactivation, regulation, and/or permeation.

Identification of the molecular determinants responsible for the proteolytic modification of $I_{Cl,swell}$-carrying VRACs in LNCaP cells described herein is even more elusive. The issue is further complicated by the fact that the molecular entity of VRACs is not known. Experimental scrutiny of three cloned proteins with quite diverse structures, CIC-2, P-glycoprotein, and pICln, considered as potential candidates for VRAC, yielded negative results (for critical reviews, see Nilius *et al.*, 1996; Okada, 1997; Strange, 1998). Another candidate that seemed quite promising until recently, ClC-3, a member of CIC family of voltage-dependent Cl^- channels (Duan *et al.*, 1997) now seems less likely. The latest evidence seriously challenges the role of CLC-3 in generating $I_{Cl,swell}$, as well as in RVD (Li *et al.*, 2000; Weylandt *et al.*, 2001), prompting researchers to look for new potential candidates.

For the Cl^--conducting channels trypsin-mediated modification has been demonstrated for endogenous CFTR (Welsh *et al.*, 1989). This modification consisted of persistent activation of the channel in excised patches by cytosolically applied trypsin, which was interpreted in terms of the removal of the regions involved in channel inactivation by the enzyme. Mutational studies of the ClC-2 channel, which exhibits cell volume-sensitivity (Gründer *et al.*, 1992) and has, therefore, been suggested as a candidate for VRAC, have shown that its gating may well function in conformity with the ball-and-chain mechanism, with the N terminal region serving as the inactivation domain and the cytoplasmic loop between transmembrane domains D7 and D8 representing the receptor site (Grunder *et al.*, 1992; Jordt and Jentsch, 1997). Deletion of the N terminal region or mutations in the D7–D8 loop abolished channel gating by swelling and/or voltage, leading to its constitutive opening.

The complex action of intracellular trypsin on $I_{Cl,swell}$ observed in our experiments suggests that VRAC determinants responsible for volume sensitivity, voltage-dependent inactivation, and permeation are intracellularly localized and are readily accessible for proteolytic cleavage. Unfortunately, since $I_{Cl,swell}$ activation by hypotonicity takes minutes, it is not possible to determine which of the current characteristics is modified first, in response to the gradual rise in trypsin concentration within the cell during dialysis, as was done for L-type Ca^{2+} current in cardiac myocytes (Hescheler and Trautwein, 1988). An assessment of this type would help to judge the relative accessibility of various determinants from the inside and, concomitantly, to draw justified conclusions about their localization.

Virtually complete elimination of $I_{Cl,swell}$ voltage-dependent inactivation by trypsin strongly suggests that, by analogy with Na^+ and K^+ channels, it may well possess a ball-and-chain or hinged-lid like structures. One may hypothesized that, similarly to ClC channels (ClC-2 and ClC-3 have been proposed for the role of VRAC), the N terminus of VRAC may represents the ball-and-chain gate, with the receptor site for the ball localized on one of the intracellular loops, as it has been suggested for ClC-2 (Jordt and Jentsch, 1997). The increase in $I_{Cl,swell}$ amplitude in response to trypsin is most probably secondary to the removal of the inactivation gate that is likely to result in an increase in open channel probability.

As the volume-sensitivity mechanisms of VRACs have not yet been identified, it is quite difficult to speculate about the nature of the determinants that are cleaved by trypsin, sensitizing thereby $I_{Cl,swell}$ to the changes in cell volume. In ClC-2 channels, for instance, the same structure determinants, namely the N terminus and the D7–D8 loop, were found to be essential for channel activation by both voltage and swelling (Grunder *et al.*, 1992; Jordt and Jentsch, 1997). It is reasonable to assume that the same is true of VRAC, and that apparent sensitization of $I_{Cl,swell}$ to changes in cell volume is a consequence of the cleavage of the whole inactivation domain that would normally exert self-inhibitory action.

It is important to note that none of the trypsin-induced effects on $I_{Cl,swell}$ in LNCaP cells were found to depend on the presence of ATP in the patch pipette. This suggests that either ATP is not important for VRAC functions in LNCaP cells at all, or that ATP binding site(s) are localized on different channel domains from those cleaved by the enzyme.

ACKNOWLEDGMENT

This work was supported in part by an INTAS-99-01248 grant.

REFERENCES

Adams, B., and Tanabe, T. (1997). *J. Gen. Physiol.* **110**, 379–389.
Armstrong, C. M. (1981). *Phys. Rev.* **61**, 644–683.
Armstrong, C. M., Bezanilla, F., and Rojas, E. (1973). *J. Physiol.* **62**, 375–391.
Armstrong, C. M., and Hille, B. (1998). *Neuron* **20**, 371–380.
Bezanilla, F., and Armstrong, C. M. (1977). *J. Physiol.* **70**, 549–566.
Catterall, W. A. (1996). *J. Bioenerg. Biomembr.* **28**, 219–230.
Duan, D., Winter, C., Cowley, S., Hume, J. R., and Horowitz, B. (1997). *Nature* **390**, 417–421.
Gonoi, T., and Hille, B. (1987). *J. Gen. Physiol.* **89**, 253–274.
Gründer, S., Thiemann, A., Pusch, M., and Jentesch, T. J. (1992). *Nature* **360**, 759–762.
Hescheler, J., and Trautwein, W. (1988). *J. Physiol.* **404**, 259–274.
Hoshi, T., Zagotta, W. N., and Aldrich, R. W. (1990). *Science* **250**, 506–507.
Jackson, P. S., Morrison, R., and Strange, K. (1994). *Am. J. Physiol.* **267**, Cl203–C1209.
Jackson, P. S., and Strange, K. (1995). *J. Gen. Physiol.* **105**, 661–676.
Jordt, S.-E., and Jentsch, T. J. (1997). *EMBO J.* **16**, 1582–1592.
Kubo, M., and Okada, Y. (1992). *J. Physiol.* **456**, 351–371.
Lemonnier, L., Prevarskaya, N., Shuba, Y., Vanden Abeele, F., Nilius, B., Mazurier, J., and Skryma, R. (2002). *FASEB J.* **16**, 222–224.
Levitan, I., and Garber, S. S. (1995). *Pflügers Arch.* **431**, 297–299.
Li, X., Shimada, K., Showalter, L. A., and Weinman, S. A. (2000). *J. Biol. Chem.* **275**, 35994–35998.
Mayorga-Wark, O., Costantin, J., Dubinsky, W. P., and Schultz, S. G. (1993). *Am. J. Physiol.* **265**, C541–C547.
Meyer, K., and Korbmacher, C. (1996). *J. Gen. Physiol.* **108**, 177–193.
Nilius, B., Eggermont, J., Voets, T., Buyse, G., Manolopoulos, V., and Droogmans, G. (1997). *Prog. Biophys. Mol. Biol.* **68**, 69–119.
Nilius, B., Eggermont, J., Voets, T., and Droogmans, G. (1996). *Gen. Pharmacol.* **27**, 1131–1140.
Oiki, S., Kubo, M., and Okada, Y. (1994). *Jpn. J. Physiol.* **44**, S77–S79.
Okada, Y. (1997). *Am. J. Physiol.* **273**, C755–C789.
Push, M., and Neher, E. (1988). *Pflügers Arch.* **411**, 201–211.
Shuba, Y. M., Hesslinger, B., Trautwein, W., McDonald, T. F., and Pelzer, D. (1990). *Pflügers Arch.* **415**, 767–773.
Shuba, Y. M., Prevarskaya, N., Lemonnier, L., Van Coppenolle, F., Kostyuk, P. G., Mauroy, B., and Skryma, R. (2000). *Am. J. Physiol.* **279**, C1144–C1154.
Skryma, R. N., Prevarskaya, N. B., Dufy-Barbe, L., Odessa, M. F., Audin, J., and Dufy, B. (1997). *Prostate* **32**, 112–122.
Solaro, C. R., and Lingle, C. J. (1992). *Science* **257**, 1694–1698.
Strange, K. (1998). *J. Gen. Physiol.* **111**, 617–622.
Strange, K., Emma, F., and Jackson, P. S. (1996). *Am. J. Physiol.* **270**, C711–C730.
Stühmer, W., Conti, F., Suzuki, H., Wang, X. D., Noda, M., Yahagi, N., Kubo, H., and Numa, S. (1989). *Nature* **339**, 597–603.
Vassilev, P. M., Scheuer, T., and Catterall, W. A. (1988). *Science* **241**, 1658–1661.
Welsh, M. J., Li, M., and McCann, J. D. (1989). *J. Clin. Invest.* **84**, 2002–2007.
Weylandt, K. H., Valverde, M. A., Nobles, M., Raguz, S., Amey, J. S., Diaz, M., Nastrucci, C., Higgins, C. F., and Sardini, A. (2001). *J. Biol. Chem.* **276**, 17461–17467.
Zagotta, W. N., Hoshi, T., and Aldrich, R. W. (1990). *Science* **250**, 568–571.
Zhang, J.-F., Ellinor, P., Aldrich, R. W., and Tsien, R. W. (1994). *Nature* **372**, 97–100.